Maritime Radio Propagation with the Effects of Ship Motions

Fang Huang, Yong Bai, and Wencai Du
College of Information Science and Technology, Hainan University, Haikou, 570228, China
Email: huang_hainu@163.com; bai@hainu.edu.cn; wencai@hainu.edu.cn

Abstract —For designing maritime wireless transmission system, the radio propagation over sea surface needs to be known first. One of the distinct characteristics of maritime radio propagation is the impact of ship motions due to the fluctuation of sea waves. This paper establishes a radio propagation model with the integration of the effects of ship motions. Using such an integrated radio propagation model, the maritime radio propagation characteristics are analyzed and discussed under different transmission distances, different carrier frequencies, and different motion types.

Index Terms—Radio propagation, Maritime communications, Channel modeling

I. Introduction

In the ship-to-ship and the ship-to-shore wireless communications over the sea, the radio signal propagates over the sea surface. Hence, the radio propagation over sea surface needs to be studied first for designing the maritime wireless transmission system. One of the distinct characteristics of maritime radio propagation is the impact of ship motions due to the fluctuation of sea waves. The angle between the transmit antenna and the receive antenna changes with ship motions, which results in the fluctuations of the received power at the receive antenna. In previous investigations on maritime radio propagation models, several deterministic models such as the Free Space Loss (FSL) model and the Plain Earth Loss (PEL) model based on Friis transmission formula and two-ray tracing method have been commonly used as references for the open-sea environment [1]-[4]. In addition, the distance between the transmitter and the receiver can be far in the maritime radio transmission environment, and the effect of the earth curvature cannot be ignored. Another deterministic path-loss model for the open-sea environment was proposed in accordance with measurements at 2 GHz with a maximum distance of 45 km [5]-[7]. The proposed model accounts for different effects including effective reflection, divergence, and diffraction due to rough sea and earth curvature. However, the abovementioned studies have not considered the effects of ship motions. Hubert et al. presented a maritime radio link channel simulator and studied the impact of ship motions with a 3D antenna gain model [8]. Therein, the numerical results of the receive power was given only for the up-down ship motion at 2.4GHz carrier frequency with a fixed transmission distance. Nevertheless, it still lacks the study of maritime radio propagation with the effects of ship motions under different transmission distances, different carrier frequencies, and different motion types. To further investigate the maritime radio propagation with the effects of ship motions, this paper first improves the traditional two-ray propagation model by taking into account the earth curvature, and then establishes a radio propagation model by integrating the 3D antenna gain model of ship motions with the improved two-ray propagation model. Using such a model, the maritime radio propagation characteristics are analyzed and discussed under different transmission distances, carrier frequencies, and different motion types.

The rest of this paper is organized as follows. Section II describes the maritime radio propagation path. Section III improves traditional two-ray propagation model by taking into account the earth curvature. Section IV establishes the radio propagation model by integrating a 3D model antenna direction gain model of ship motions with the improved two-ray propagation model. Section V presents the numerical results of the radio propagation with the effects of ship motions using the established model. Section VI concludes this paper.

II. Maritime Radio Propagation Path

Frist, we discuss the radio propagation path over sea surface. For over-the-sea transmission to and from ships, the effect of earth curvature on the radio propagation needs to be taken into account. Fig. 1 illustrates the radio propagation path over sea surface between a terminal on ship and a base station on land. The ship-to-shore radio propagation distance can be divided into three segments according to the distance between the RF transmitter and receiver: segment A, which is from T (the point of the base station) to R_A (the sightline of the base station) with length d_1; segment B, which is from R_A to R_B (the sightline of the terminal) with length d_2; and segment C, which is the shadow area beyond R_B [9]. Segment A is a line-of-sight path through free space, with no obstacles nearby to cause reflection or diffraction. In the segment B and C, diffraction arises because of the curved way in which waves propagate.

Manuscript received January 12, 2015; revised May 13, 2015.
Corresponding author: Wencai Du, email: wencai@hainu.edu.cn
doi:10.12720/jcm.10.5.345-351

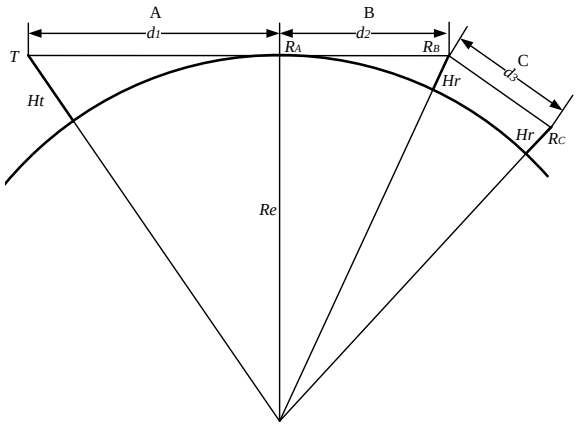

Fig. 1. Three distance segments of maritime radio propagation

Assume that the antenna heights of base station and terminal are H_t, and H_r, respectively. Using trigonometry, it can be calculated that [10]

$$d_1^2 + R_e^2 = (H_t + R_e)^2 \tag{1}$$

$$d_1 = \sqrt{2R_e H_t + H_t^2} \tag{2}$$

where R_e is the earth radius, and R_e=8500km. Because $R_e >> H_t$, we can get

$$d_1 = \sqrt{2R_e H_t} \tag{3}$$

Similarly,

$$d_2 = \sqrt{2R_e H_r} \tag{4}$$

III. Improved Two Ray Propagation Model

The reflection effect from the sea surface and the scattering effect due to the roughness of sea waves result in multipath components of the transmitted signal at the receive antenna. The random phase and amplitudes of different multipath components cause fluctuations in signal strength [11]. In [12], the roughness factor judgment, Rayleigh judgment, coherent reflection coefficient method and specular and diffuse reflection coefficients method are used to analyze the reflection characteristics of electromagnetic waves over the sea. It is concluded that the sea surface can be assumed smooth mirror surface when the sea state is seven and the grazing angle is from 0 to 1.3 degrees, or the sea state is six and the grazing angle is from 0 to 2.5 degrees. This paper assumes that the sea surface is calm, and only considers the effect of specular reflection. Thus, a two-ray model can be used for analyzing the radio propagation over sea surface. As shown in Fig. 2, a two-ray model of radio propagation includes a direct path and a specular reflection path. The direct signal path is the line of sight (LOS) signal propagation between the transmitter and the receiver. The specular reflection path is produced by the reflection from the smooth sea surface [13].

To make the model more precise, we modify the two-ray model considering the earth curvature as shown in Fig. 2. In general, the distance between the transmitter and the receiver, R_d can be calculated according to the time delay, then the value of α can be calculated by

$$\alpha = \cos^{-1}\left(\frac{(h_t + R_e)^2 + (h_r + R_e)^2 - R_d^2}{2(h_t + R_e)(h_r + R_e)}\right) \tag{5}$$

In [14], l_1 can be calculated by the flowing formula when we assume the height and size of the antenna is much smaller than the earth radius,

$$2l_1^3 - 3ll_1^2 + (l^2 - 2R_e(h_r + h_t))l_1 + 2R_e h_r l = 0 \tag{6}$$

The value of α_1 and α_2 can be calculated by

$$\alpha_1 = l_1 / R_e \tag{7}$$

$$\alpha_2 = (l - l_1) / R_e \tag{8}$$

Then, R_1 and R_2 can be calculated by

$$R_1 = \sqrt{R_e^2 + (R_e + h_t)^2 - 2R_e(R_e + h_t)\cos\alpha_1} \tag{9}$$

$$R_2 = \sqrt{R_e^2 + (R_e + h_r)^2 - 2R_e(R_e + h_r)\cos\alpha_2} \tag{10}$$

Finally, in [13], the grazing angle considering the earth curvature can be calculated by

$$\varphi_g = \sin^{-1}\left(\frac{h_r}{R_2} - \frac{R_2}{2R_e}\right) \tag{11}$$

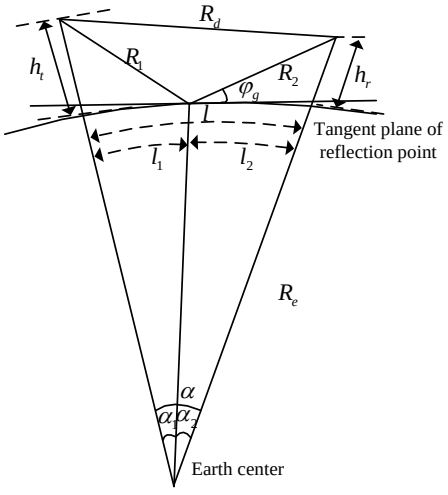

Fig. 2. Two-ray model considering the earth curvature

IV. Integrated Martime Radio Propagation Model with Ship Motions

A. Ship Motion Modeling

Surface fluctuations are generally divided into three types: waves caused by wind, tidal caused by gravity and centrifugal force, and the tsunami caused by tectonic. This paper only considers the wave motions caused by wind [15]. The directions of ship motions can be up and down, left and right, front and rear. It can be described

with the motion model $(x, y, z, \alpha, \beta, \gamma)$ of six degrees of freedom [16]. A 3D coordinate system (x, y, z), in which O is the Earth center, is shown in Fig. 3. Heave is a translation along z axis (up and down), and roll is a rotation about x axis (left and right), and pitch is a rotation about y axis (front and rear).

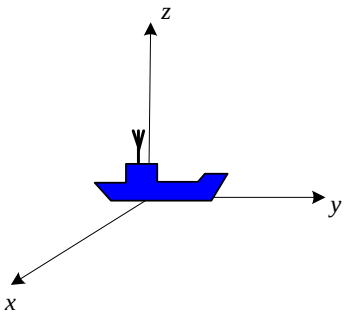

Fig. 3. ship in 3D coordinate system

The variation range of the heave motion is H_{max} which is the crest-to-trough wave height. The variation ranges of both the pitch motion and the roll motion can be expressed by $\theta_{\max}$, which is the antenna maximum angular deviation from vertical direction, as show in Fig. 4. Without real ship motion records, approximate geometrical relations can be derived for $\theta_{\max}$. It can be calculated by

$$\theta_{\max} = \arcsin\left(\frac{\pi H_{\max}}{\sqrt{\lambda_s^2 + \pi^2 H_{\max}^2}}\right) \tag{12}$$

where λ_s is the wavelength of sea wave. Using the fundamental mode of the Pierson-Moskowitz spectrum for fully developed regular wind waves [17], a complete data set is defined for the studied case. It includes the period $T_s \approx 7$s, and $\lambda_s \approx 131.4$m. At the sea condition Douglas 5, H_{max} is about 5.7m. According to (12), we can get $\theta_{max} = 7.7°$.

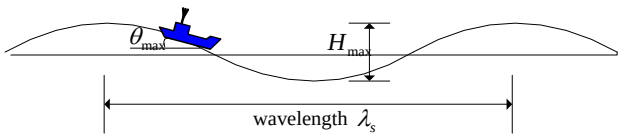

Fig. 4. Variation ranges of sea waves

B. Integrated Propagation Model with the Effects of Ship Motions

Then we analyze the change of antenna gains of the transmitter and receiver when ships move on the sea surface. A radiation vector function $\boldsymbol{G}$ is introduced to account for the polarization state and the antenna gain along any direction [18]. $G(\theta, \phi)$ depends on the realized gain for a given set of departure (emitting antenna) or arrival (receiving antenna) angles,

$$\boldsymbol{G} = \sqrt{G(\theta,\phi)}\boldsymbol{U} = \sqrt{G(\theta,\phi)}\begin{pmatrix} U_\theta(\theta,\phi) \\ U_\phi(\theta,\phi) \end{pmatrix} \tag{13}$$

where θ and ϕ are elevation angle and azimuth angle, respectively. As shown in Fig. 5, $\boldsymbol{U}$ is a normalized vector which corresponds to the strength ratio emitted (or received) along $\overrightarrow{U_\theta}$ and $\overrightarrow{U_\phi}$ components. A database of antenna gains for simulation can be created using HFSS, an electromagnetic (EM) simulator.

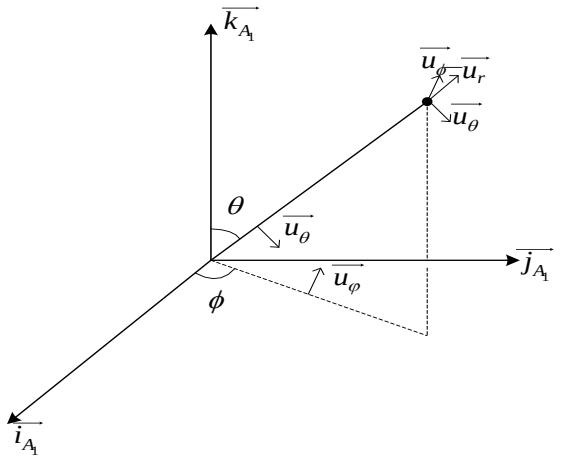

Fig. 5 Antenna coordinate system

In the coordinate system, the direct-path channel matrix C_D can be calculated by

$$C_D = \frac{1}{R_d}\sqrt{G^A}\sqrt{G^B}\begin{pmatrix} U_\theta^B & U_\phi^B \end{pmatrix}\cdots \cdot\begin{pmatrix} \vec{u}_\theta^A\cdot\vec{u}_\theta^B & \vec{u}_\phi^A\cdot\vec{u}_\theta^B \\ \vec{u}_\theta^A\cdot\vec{u}_\phi^B & \vec{u}_\phi^A\cdot\vec{u}_\phi^B \end{pmatrix}\cdot\begin{pmatrix} U_\theta^A \\ U_\phi^A \end{pmatrix} e^{-j2\pi R_d/\lambda} \tag{14}$$

where $\overrightarrow{u_\theta}$ and $\overrightarrow{u_\varphi}$ present the unit vectors along the angles of θ and φ.

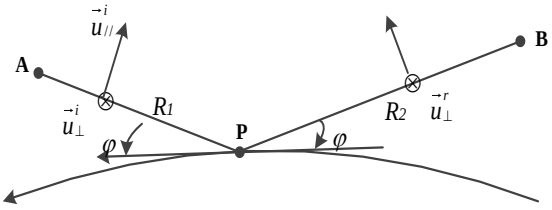

Fig. 6. Unit vector definition for specular reflection

The reflected-path channel matrix C_R can be calculated by

$$C_R = \frac{1}{R_1+R_2}\sqrt{G^A}\sqrt{G^B}\begin{pmatrix} U_\theta^B & U_\phi^B \end{pmatrix}\cdots \cdot\begin{pmatrix} \vec{u}_\theta^B\cdot\vec{u}_{//}^r & \vec{u}_\theta^B\cdot\vec{u}_\perp^r \\ \vec{u}_\phi^B\cdot\vec{u}_{//}^r & \vec{u}_\phi^B\cdot\vec{u}_\perp^r \end{pmatrix}\cdot\rho_{FD}\cdot\rho_r\cdot\begin{pmatrix} \rho_{//} & 0 \\ 0 & \rho_\perp \end{pmatrix}\cdots \cdot\begin{pmatrix} \vec{u}_\theta^A\cdot\vec{u}_{//}^r & \vec{u}_\phi^A\cdot\vec{u}_{//}^r \\ \vec{u}_\theta^A\cdot\vec{u}_\perp^r & \vec{u}_\phi^A\cdot\vec{u}_\perp^r \end{pmatrix}\cdot\begin{pmatrix} U_\theta^A \\ U_\phi^A \end{pmatrix}\cdot e^{-j2\pi(R_1+R_2)/\lambda} \tag{15}$$

where $\vec{u}_{//}^{\,r}$ and $\vec{u}_\perp^{\,r}$ are shown in Fig. 6; ρ_{FD} is the factor of energy dispersion [19] and it can be calculated by

$$\rho_{FD}=\left(1+\frac{2R_1R_2}{R_e(R_1+R_2)\sin\varphi_g}\right)^{-1/2}\left(1+\frac{2R_1R_2}{R_e(R_1+R_2)}\right)^{-1/2} \quad (16)$$

For predicting the specular reflection coefficient ρ_r, Ament presented in [20] that it can be calculated by

$$\rho_r=\exp\left(-2(2\pi g)^2\right)\cdot I_0\left(2(2\pi g)^2\right) \quad (17)$$

$$g=(\sigma_h\sin\varphi_g)/\lambda \quad (18)$$

where σ_h is the rms surface height variation, φ_g is the grazing angle of incident, λ is the wavelength, and I_0 represents the modified Bessel function of zero order.

Next, the power strength at the receiver can be calculated as

$$\begin{aligned}P(dB)&=10\log_{10}\frac{P_r}{P_t}=10\log_{10}\left(\left(\frac{\lambda}{4\pi}\right)^2\left|C_D+C_R\right|^2\right)\\&=20\log_{10}\left(\left(\frac{\lambda}{4\pi}\right)\left|C_D+C_R\right|\right)\end{aligned} \quad (19)$$

In segment A, two-ray radio propagation model is used for analysis. In segment B, one-ray model can be used since the reflected path can be ignored. The propagation path losses for segment A and B can be written as

$$\begin{aligned}L_a&=147.5582-20\lg f+\beta(f,d)\\&=147.5582-20\lg f+20\lg\left|C_{DP}+C_{RP}\right|\end{aligned} \quad (20)$$

$$L_b=147.5582-20\lg f+20\lg\left|C_{DP}\right| \quad (21)$$

We also can obtain the direct-path channel matrix C_D without motions by the following equations,

$$C_D=\frac{1}{R_d}\sqrt{G^A}\sqrt{G^B}\begin{pmatrix}U_\theta^B & U_\phi^B\end{pmatrix}\begin{pmatrix}U_\theta^A\\U_\phi^A\end{pmatrix}e^{-j2\pi R_d/\lambda} \quad (22)$$

In the same way, we obtain the reflected-path channel matrix C_R without motions by the following equations,

$$\begin{aligned}C_R=&\frac{1}{R_1+R_2}\sqrt{G^A}\sqrt{G^B}\begin{pmatrix}U_\theta^B & U_\phi^B\end{pmatrix}\rho_{FD}\cdot\rho_r\cdots\\&\cdot\begin{pmatrix}\rho_{//} & 0\\0 & \rho_\perp\end{pmatrix}\begin{pmatrix}U_\theta^A\\U_\phi^A\end{pmatrix}\cdot e^{-j2\pi(R_1+R_2)/\lambda}\end{aligned} \quad (23)$$

V. Numerical Results

In this section, we study the maritime radio propagation characteristics under different transmission distances, different carrier frequencies, and different motion types (heave, roll, and pitch) by using the integrated radio propagation model presented in Section IV.

We assume the antennas at the transmitter and receiver for wireless communications are both half-wavelength dipole antennas with maximum gain 2.1 dBi. The heights of transmitter and receiver are both 10m. With such assumptions, the range of segment A is 13 km, and the segment B is 23 km according to (1) to (4). Furthermore, we assume that the transmitter is on the shore, when the receiver is located in the sea, and the distance between them is set to 1 km, 5 km, 10 km and 20 km, respectively. Finally, we suppose that the sea condition is Douglas 5, and the surface fluctuation cycle is 7 seconds.

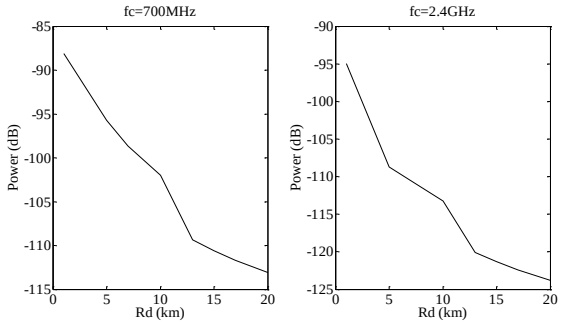

Fig. 7. Received power versus transmission distance when ship is motionless

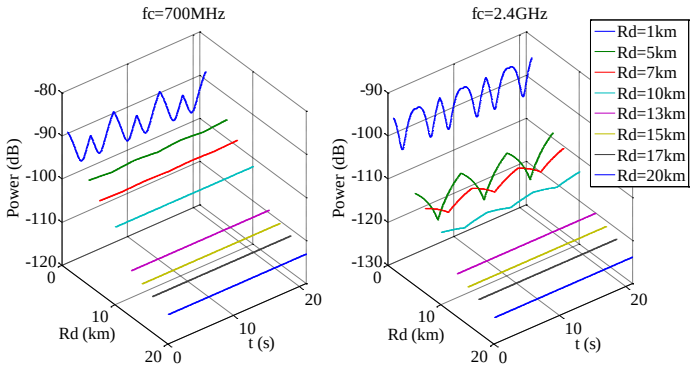

Fig. 8. Received power versus time and transmission distance with ship heave (up and down) motion

Using the integrated radio propagation model, we present the numerical results of maritime radio propagation under different transmission distances, different carrier frequencies (700 MHz and 2.4 GHz), and three motion types (heave, roll, and pitch). The numerical results are shown in Fig. 7 to Fig. 11.

Fig. 7 shows the received power versus the transmission distance for f_c=700MHz and f_c= 2.4GHz without ship motions. Figure 8 shows the received power versus time and the transmission distance for f_c=700MHz and f_c= 2.4GHz under ship heave (up and down) motion. The horizontal distance between the transmitter and

receiver is from 1km to 20km. It can be seen that with the increase of transmission distance, the fluctuations of received power become smaller, which implies that the impact of ship motions on radio propagation become smaller at far transmission distance.

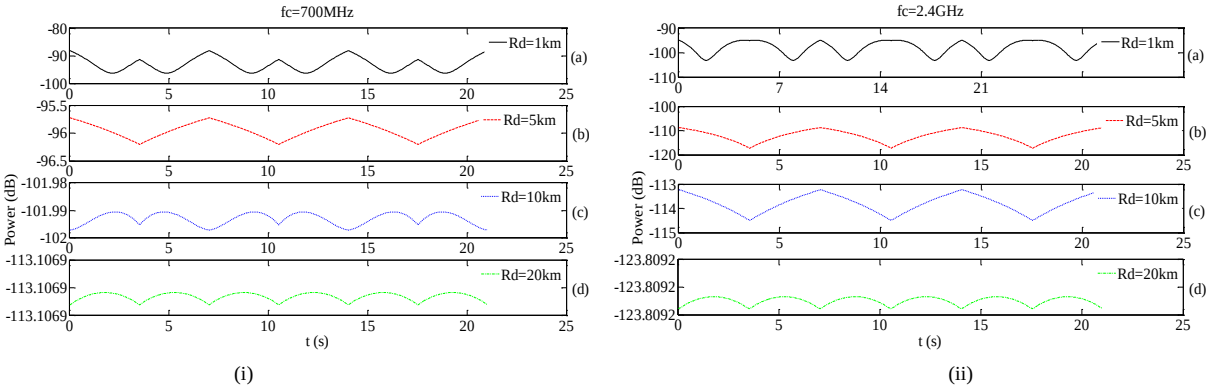

Fig. 9. Received power versus time at different transmission distances with ship heave (up and down) motion

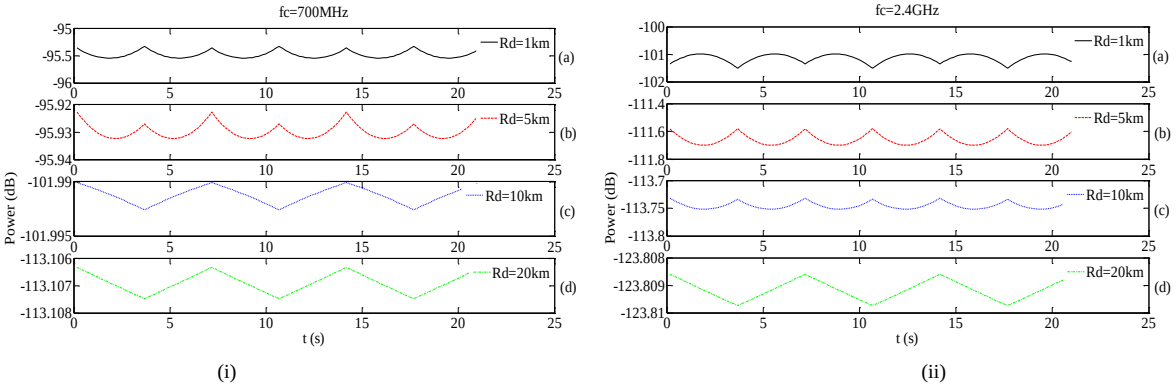

Fig. 10. Received power versus time at different transmission distances with ship roll (left and right) motion

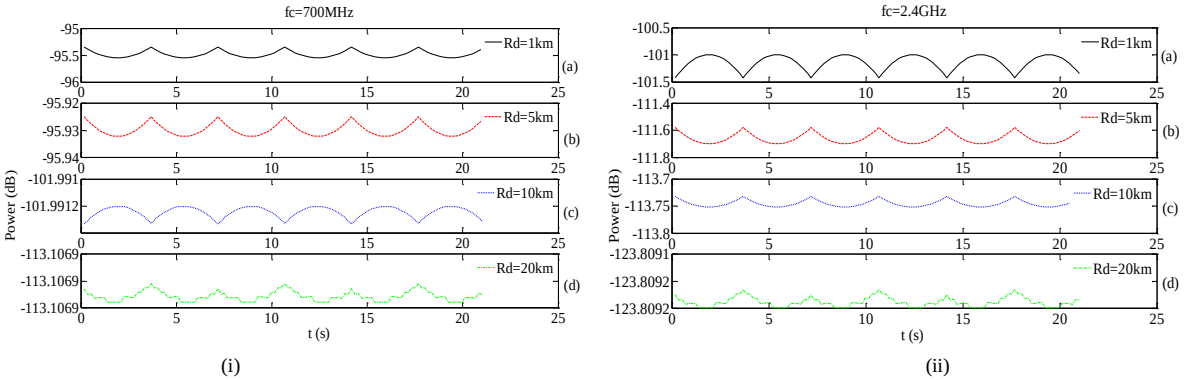

Fig. 11. Receiver power versus time at different transmission distances with ship pitch (front and rear) motion

Fig. 9, Fig. 10, and Fig. 11 show the receiver power versus time at different transmission distances under ship heave, roll, and pitch motions, respectively. In these figures, the propagation model equation of segment A is used when the transmission distance is 1*km*, 5*km* and 10*km*; the propagation model equation of segment B is used when the transmission distance is 20*km*, which is longer than 13 km (the boundary point of segment A and B). Comparing the sub-graph (a) in Fig. 9, Fig. 10, and Fig. 11, we observe that the power loss caused by ship motions of roll and pitch is lower than that caused by heave motions. As shown in Fig. 9-i(a) and Fig. 9-ii(a), the power loss resulted from heave motion is about 9 dB, and the power loss resulted from the ship motions of roll and pitch is only about 0.2 dB. Therefore, the heave motion has the largest impact on the transmission path loss for maritime radio propagation compared to the other two motion types.

Comparing the sub-graph (d) in Fig. 9 to 11 where the transmission distance locates in Segment B, we observe that the fluctuations of received power are all relatively small under three motion types. Thus, the effects of ship motions on the received power are relatively small in Segment B, and can be negligible.

Comparing with the received powers at carrier frequencies of 700MHz and 2.4GHz, we can see that the

fluctuations of received power become larger at higher carrier frequency. Thus, the impact of ship motions on the radio propagation is more significant at higher carrier frequencies. For instance, as shown in Fig. 9-i-(a) and Fig. 9-ii-(a), when the transmission distance is 1km, the fluctuation of received power is about 9dB at 700MHz, and the fluctuation of received power is about 16dB at 2.4GHz.

VI. Conclusions

To study the maritime radio propagation with the effects of ship motions, this paper first modified traditional two-ray propagation model by taking into account the earth curvature, and then established a radio propagation model by integrating a 3D model antenna direction gain model of ship motions with the improved two-ray propagation model. Using such an integrated radio propagation model, the received power with the impact of ship motions can be obtained under different transmission conditions. From the numerical results, we analyzed the radio propagation at different transmission distances and carrier frequencies under different motion types. We draw the conclusions that the impact of ship motions on radio propagation becomes smaller with the increase of transmission distance, and the impact of ship motions on the radio propagation is more significant at higher carrier frequencies; Lastly, the heave (up and down) motion has the largest impact on the transmission path loss for maritime radio propagation compared to other two motion types.

Acknowledgment

This paper was supported by the National Natural Science Foundation of China (Grant No. 61062006 and Grant No. 61261024) and the Special Social Service Project Fund of Hainan University, China (Grant No.HDSF201301).

References

[1] N. H. Lu, "Linearized, unified two-ray formulation for propagation over a Plane Earth," in *Proc. Sensor for Industry Conference*, 2005.

[2] J. Joe, S. K. Hazra, S. H. Toh, W. M. Tan, and J. Shankar, "Path loss measurements in sea port for WiMAX," in *Proc. IEEE Conference on Wireless Communications and Networking Conference*, 2007.

[3] ITU-R Recommendation P.1546-2, "Method for point-to-area predictions for terrestrial services in the frequency range 30 MHz to 3000 MHz," Sep. 2005.

[4] L. J. Zhang, H. G. Wang, R. Zhang, *et al*., "Radio wave propagation characteristics measurement and modeling over the sea," in *Proc. General Assembly and Scientific Symposium (URSI GASS)*, 2014, pp. 1-4.

[5] K. Yang, T. Roste, F. Bekkadal, and T. Ekman, "Experimental multipath delay profile of mobile radio channels over sea at 2 GHz," in *Proc. Antennas and Propagation Conference (LAPC)*, 2012, pp. 1-4.

[6] K. Yang, T. Roste, F. Bekkadal, *et al*., "Long-distance propagation measurements of mobile radio channel over sea at 2 GHz," in *Proc. IEEE Vehicular Technology Conference (VTC Fall)*, 2011, pp. 1-5.

[7] K. Yang, A. F. Molisch, T. Ekman, and T. Roste, "A deterministic round earth loss model for open-sea radio propagation," in *Proc. IEEE Vehicular Technology Conference (VTC Spring)*, 2013, pp. 1-5.

[8] W. Hubert, Y. M. Le Roux, M. Ney, *et al*., "Impact of ship motions on maritime radio links," *IEEE Trans. International Journal of Antennas and Propagation*, vol. 2012, pp. 1-6, Nov.2012.

[9] Y. S. Meng and Y. H. Lee, "Measurements and characterizations of air-to-ground channel over sea surface C-band with low airborne altitudes," *IEEE Transaction on Vehicular technology*, vol. 60, no. 4, pp. 1943-1948, 2011.

[10] T. S. Rappaport, *Wireless Communications: Principles and Practice*, Prentice Hall, January, 2002, pp. 23-50.

[11] F. P. Fontan and A. Rocha, "Estimation of the number of clusters in multipath radio channel data sets," *IEEE Transactions on Antennas and Propagation*, vol. 61, no. 5, pp. 2879-2883, 2013.

[12] M. Dong, Y. B. Zhao, and S. H. Zhang, "The analysis of the multipath model under the VHF band and at sea," *Acta Electronic Sinica*, vol. 36, no. 6, pp. 1373-1377, 2009.

[13] X. Q. Hu, J. B. Chen, and Y. L. Wang, "Research on metre-wave radar height-finding multipath model," *Chinese Journal of Radio Science*, vol. 23, no. 4, pp. 651-657, 2008.

[14] B. R. Mahafza, *Radar Systems Analysis and Design Using MATLAB*, Boca Raton: CRC Press, 2000.

[15] A. Fung and K. Lee, "A semi-empirical sea-spectrum model for scattering coefficient estimation," *IEEE Transaction on Oceanic engineering*, vol. 7, no. 4, pp. 166-176, 1982.

[16] X. Yang and X. H. Wang, "Modeling and simulation research of six-degree-of-freedom fighter," *Journal of System Simulation*, vol. 12, no. 3, pp. 210-213, 2000.

[17] L. Gardenal, B. Philibert, and R. M. Turner, "Study of the interaction of electromagnetic waves on a sea surface: Improvement of the algorithm of low-altitude tracking of radar targets," in *Proc. Canadian Conference on Electrical and Computer Engineering*, vol. 2, pp. 693–696, 1994.

[18] B. Uguen, L. M. Aubert, and F. T. Talom, "A comprehensive MIMO-UWB channel model framework for ray tracing Approaches," in *Proc. IEEE Ultra-Wideband Conf.*, 2006, pp. 231-236.

[19] R. J. Papa, J. F. Lennon, and R. L. Taylor, "Multipath effects on an azimuthal monopulse system," *IEEE Transactions on Aerospace and Electronic System*, vol. 19, no. 4, pp. 585-597, July 1983.

[20] A. R. Miller, R. M. Brown, and E. Vegh, "New derivation for the rough-surface reflection coefficient and for the distribution of sea-wave elevation," in *Proc. IEEE H(Microwaves, Optics and Antennas)*, vol. 131, no. 2, pp. 114-116,1984.

Fang Huang received the B.S. degree from Anhui Normal University, China, in 2012. She is currently pursuing her M.S. degree at the College of Information Science & Technology, Hainan University. Her research interests include radio channel modeling, and wireless communications.

Yong Bai received his B.S. degree from Xidian University, China, in 1992, and M.S. degree from Beijing University of Posts and Telecommunications (BUPT), China, in 1995, and Ph.D. degree from Rutgers-The State University of New Jersey in 2001. He was with PacketVideo Corporation from 2000 to 2002. He was with Motorola from 2002 to 2004. He was with CEC Wireless from 2004 to 2005. He was a senior researcher at DOCOMO Beijing

Communication Labs from 2005 to 2009. He is a professor at College of Information Science & Technology, Hainan University since 2010. He acted as the Lead Guest Editor for EURASIP Journal on Wireless Communications and Networking, Special Issue on Topology Control in Wireless Ad Hoc and Sensor Networks. His current research interests include mobile communications, and maritime communications. He is a member of the IEEE.

Wencai Du received the B.S. degree from Peking University, China, two M.S. Degrees from ITC, The Netherlands, and Hohai University, China, respectively, and Ph.D. degree from South Australia University, Australia. He was a Post-doctor Fellow in Israel Institute of Technology (IIT), Haifa, Israel. He is Dean of College of Information Science & Technology at Hainan University and Director of Maritime Communication and Engineering of Hainan province. He has authored or coauthored 18 books and more than 80 scientific publications. He is currently members of the Editorial Board of Inverts Journal of Science and Technology, India. He has taken services on many professional conferences, including Conference Chair of IEEE/ACIS ICIS 2011, Conference Co-Chair of IEEE/ACIS SNPD 2010, London, Conference Chair of IEEE/ACIS SERA 2009, and Program Chair of IEEE/ACIS SNPD 2009, Daegu, Korea. His research interests include several aspects of Information Technology and Communication (ITC), including computer network and maritime communications.